

ACCURATE TOP OF THE ATMOSPHERE ALBEDO DETERMINATION FROM MULTIPLE VIEWS OF THE MISR INSTRUMENT

Christoph C. Borel, Siegfried A. W. Gerstl

NIS-2, Mailstop C323,
Los Alamos National Laboratory,
Los Alamos, NM 87545, USA
cborel@lanl.gov, <http://nis-www.lanl.gov/~borel/>

Abstract— Changes in the Earth’s surface albedo impact the atmospheric and global energy budget and contribute to global climate change. It is now recognized that multi-spectral and multi-angular views of the Earth’s top of the atmosphere (TOA) albedo are necessary to provide information on albedo changes. In this paper we describe one semi-empirical bidirectional reflectance factor (BRF) model based on the “Coupled Surface-Atmosphere Reflectance” (CSAR) model which is inverted for two unknowns. The retrieved BRF parameters are then used to compute the TOA spectral albedo for clear sky conditions. Using this approach we find that the albedo can be computed with better than 1% error in the visible and 1.5% in the near infrared (NIR) for most surface types.

1. INTRODUCTION

The Multi-angle Imaging Spectro-Radiometer (MISR) instrument is slated for the EOS-AM platform to be launched in 1998. The instrument consists of nine cameras pointed at zenith angles of ± 70.5 , ± 60 , ± 45 , ± 26.1 and 0 degrees in the along track direction. Each camera has four spectral channels with center bandpass wavelengths at 443 nm (blue), 550 nm (green), 670 nm (red) and 865 nm (near infrared). The instrument will be used to infer top of the atmosphere spectral albedo (clear and cloudy conditions), surface bidirectional reflectance, global aerosol distributions and other atmosphere and surface parameters at the 4 spectral bands. Global monitoring of the earth radiation budget is one of the main goals in global change research programs. Thus global measurements of the TOA albedo are important (Kimes and Sellers, 1985). Our goal is to compute the TOA spectral albedo for clear sky conditions from MISR measurements (Diner et al., 1994).

1.1. Definition of the TOA Albedo

The albedo in each MISR channel c , $c = [1, 2, 3, 4]$ is defined as:

$$\alpha_{0,c}(\mu_s) = \frac{1}{\pi} \int_0^1 d\mu_v \mu_v \int_0^{2\pi} d\phi_v BRF_c(\mu_s, \mu_v, \phi_v),$$

with the notation: $\alpha_{0,c}(\mu_s)$ is the top of atmosphere albedo in MISR channel c , ϕ_v is the angle relative to the solar azimuth, μ_s is the cosine of the solar zenith angle θ_0 , μ_v is the cosine of the view zenith angle θ and $BRF_c(\mu_s, \mu_v, \phi_v)$ is the bidirectional reflectance factor in MISR channel c (Nicodemus et al, 1977). The relationship between the *BRF* and the bidirectional reflectance distribution function *BRDF* is

$$BRDF_c(\mu_s, \mu_v, \phi_v) = \frac{1}{\pi} BRF_c(\mu_s, \mu_v, \phi_v).$$

The BRF_c is related to the radiance L_c by the following equation

$$BRF_c(\mu_s, \mu_v, \phi_v) = \frac{\pi L_c(\mu_s, \mu_v, \phi_v) D^2}{\mu_s E_{0,c}},$$

where $D = R(t)/R_0$ is the normalized distance to the sun. $R(t)$ is the time dependent distance and R_0 is the distance for which E_0 is defined and E_0 is the TOA solar irradiance.

For each channel, MISR has nine cameras that measure the BRF at nadir and at four different off nadir zenith in two different azimuthal angles (forward and aft). Since we have only two azimuthal measurements for each off nadir zenith angle we need an azimuthal model to interpolate between the MISR measurements. This model has to be true for different surface cover types and for various atmospheric conditions. Thus, to find an appropriate AZM we compute the $BRF_c(\mu_s, \mu_v, \phi_v)$ and the TOA albedo $\alpha_{0,c}(\mu_s)$ for a number of model cases.

2. SIMULATED MISR DATA SET

Since there is no MISR data yet available it was necessary to simulate MISR data as closely as possible to what is

expected from the EOS instrument in a few years. Several “Radiative transfer” (RT) codes were considered for this task. A key requirement was that the surface had to be modeled using a surface “Bidirectional Reflectance Distribution Function” (BRDF) (e.g. Nicodemus et al, 1977). Furthermore the RT codes must accurately calculate the multiple scattering for a large range of sun and view angles in order to perform a numerical integration over the hemispherical BRDF for the albedo calculation. Multiple scattering is an important component of the measured signal in the visible and near infrared spectral region.

We considered and used two available codes - 6S (Vermeete et al, 1994) and JMRT (Martonchik, 1994). The RT code MODTRAN3 was not used yet since it was not available prior to this work (Abreu et al, 1995).

2.1. The “John Martonchik Radiative Transfer” (JMRT) Code

Using a radiative transfer code written by John Martonchik at JPL we generated hemispherical TOA radiance fields for four MISR channels, five different aerosol types (urban, rural, maritime, desert and arctic) and 46 surface BRDF’s from experimental data and models for vegetation (23), bare soil (3), rough water surface (11), snow and ice (9).

In the original JMRT output, the BRDF values are given only at the MISR camera angles. In two slightly different versions we compute the BRDFs for the following quadrature zenith angles : 77.00°, 65.0°, 52.50°, 37.00°, 0.00° (version 1) and 85.00°, 70.50°, 60.00°, 45.60°, 26.10° (version 2). Note that the underlined zenith quadrature angles are also the MISR camera zenith angles.

In addition to these changes the JMRT code is now able to read any given BRDF model directly from a modified BRDF subroutine instead of having an additional subroutine for the Kimes data only (Kimes and Sellers, 1985). Any measured BRDF can be entered as well, given that it has been measured at certain view angles and sun angles.

We have set up a driver program written in IDL to create the input parameters for JMRT and to compute TOA BRDF values at the 10 zenith and at 12 relative azimuthal quadrature angles (0°, 30°, ... , 330°).

Using the computed angular-dependent hemispherical data we can compute a “true” TOA albedo $\alpha_{0,c}(\mu_s)$ based on fine scale RT calculations in $N_\phi = 12$ azimuthal and $N_\theta = 10$ elevation angles.

3. AZIMUTHAL MODELS FOR THE TOP OF THE ATMOSPHERE REFLECTANCE

3.1. Purpose of an Azimuthal Model

Since MISR measures only in nine discrete directions it is necessary to estimate the TOA radiance in directions

which are not seen by MISR using what we call an azimuthal model (AZM). Various AZM’s were considered in this study and used to compute an albedo estimate $\widehat{\alpha_{0,c}}$. The basic idea is to take a semi-empirical function which is able to represent many different TOA BRFs. This function should have as few parameters as possible, be uniquely invertible and reciprocal (sun and view angles are interchangeable without changing the value) and should have little sensitivity to noise.

3.2. The CSAR Model

As a starting point we decided to investigate the “Coupled Surface-Atmosphere Reflectance” (CSAR) model further. In Rahman et al., 1993 the following semi-empirical model is suggested to model BRFs of terrestrial surfaces:

$$BRF_{CSAR}(\theta_s, \phi_s; \theta_v, \phi_v) = \varrho_0 \frac{\mu_s^{\kappa-1} \mu_v^{\kappa-1}}{(\mu_s + \mu_v)^{1-\kappa}} F(g) [1 + R(G)], \quad (1)$$

where ϱ_0 and κ are empirical surface parameters between 0 and 1 with the condition on ϱ_0 that the albedo of eq.(1) is between 0 and 1, and

$F(g)$ is the Henyey-Greenstein function:

$$F(g) = \frac{1 - \Theta_0^2}{[1 + \Theta_0^2 - 2\Theta_0 \cos(\pi - g)]^{1.5}}$$

Θ_0 controls the forward ($0 \leq \Theta_0 \leq 1$) and backward ($-1 \leq \Theta_0 \leq 0$) scattering peak,

g is a phase angle and given by: $\cos g = \mu_s \mu_v + \sin \theta_s \sin \theta_v \cos(\phi_s - \phi_v)$,

$(1 + R(G))$ approximates the hot-spot with:

$$1 + R(G) = 1 + \frac{1 - \varrho_0}{1 + G},$$

$$G = \sqrt{\tan^2 \theta_s + \tan^2 \theta_v - 2 \tan \theta_s \tan \theta_v \cos(\phi_s - \phi_v)}.$$

In Fig. 1 we show a polar representation of the BRDF for variable Θ_0 and κ . The center of each circle represents nadir. The radial direction is given by $\sin \theta$. The principal plane (plane in which the solar vector and the surface normal lie) is along the horizontal axis with the sun position on the right side.

3.3. Uniqueness

To test whether a BRDF model is invertible we wrote an IDL program to create many different BRDF slices similar to MISR data using the CSAR semi-empirical function for randomly chosen parameters ϱ_0 , κ and Θ_0 . A non linear least squares fitting routine (CURVEFIT.PRO) was

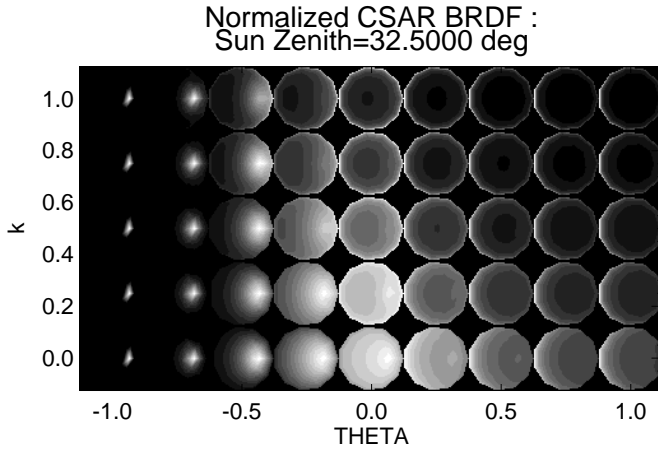


Figure 1: Polar representation of the CSAR BRDF for $\theta_s = 32.5^\circ$ and $\varrho_0 = 0.2$ as a function of Θ_0 and κ ($\alpha < 1$).

used to invert the BRDF slices and compare the retrieved parameters $\widehat{\varrho}_0$, $\widehat{\kappa}$ and $\widehat{\Theta}_0$ with the original set ϱ_0 , κ and Θ_0 . No case was observed where another solution was found. While this is not a mathematical proof that the CSAR BRDF is unique, it is sufficient for our purposes.

3.4. Noise Sensitivity

Next we investigated how much noise could be tolerated and how the albedo error changes as a function of added noise. We found that the albedo error was less than $\pm 5\%$ for $\sigma \leq 0.1$ for an albedo of 0.43. Thus there is a linear degradation of the albedo with standard deviation. Similarly the error between original and retrieved BRDF parameters grows with increased noise.

4. CLEAR SKY TOP OF ATMOSPHERE ALBEDO ALGORITHM

4.1. Algorithm Outline

The following algorithm was implemented and tested on simulated MISR BRDFs over many surface types and atmospheric conditions (channel index c is suppressed):

1. Read TOA BRDFs from JMRT output.
2. For all N_c cases $k = 1, 2, 3, \dots, N_c$ do:
 - (a) Compute the albedo $\alpha_{0,k}$
 - (b) For view azimuthal angles $\phi_j = [0^\circ, 30^\circ, 60^\circ, 90^\circ]$ do:
 - i. Extract a BRDF slice (BRF_i , $i = 1, 2, \dots, 9$) at the MISR angles for $(\phi_j, \phi_j + 180^\circ)$.

- ii. Perform nonlinear curve fit of $BRF_{j,i}$ results in estimated CSAR parameters $\widehat{\varrho}_{0,j,k}$, $\widehat{\kappa}_{j,k}$ and $\widehat{\Theta}_{0,j,k}$.

- iii. Do a numerical integration of CSAR model over the hemisphere results in estimated albedo $\widehat{\alpha}_{0,j,k}$.

- iv. Compute albedo error $\varepsilon(\alpha_{0,j,k}) = \alpha_{0,k} - \widehat{\alpha}_{0,j,k}$.

- (c) Plot standard deviation σ of the albedo error $\varepsilon(\alpha_{0,j,k})$ as a function of view azimuth ϕ_j .

- (d) Generate TOA BRDF from estimated CSAR parameters and display next to original.

3. Generate scatter plots of standard deviation of the albedo error versus azimuth marking different surface types with symbols.

5. RESULTS

Various retrieval schemes will be discussed in the next 4 sub-sections using the same TOA-BRDF data set. The standard deviation σ of the albedo error was computed over all cases dividing them into general surface classes of: Δ Vegetation (23 models), \diamond Soil and sand (3 models), $+$ Snow and ice (9 models) and $*$ Water (11 models), where the plot symbols shown will be used in Figure 2. Each surface model was used in 5 different atmospheres and 3 sun angles. Thus a total of 690 TOA BRDFs were inverted for 4 different azimuthal angles at $(0^\circ, 30^\circ, 60^\circ$ and $90^\circ)$. Including all 4 channels this data set grows to 2760 cases. This process (with visualization of the original and fitted BRDFs in polar surface plots) took about one hour on a Sparc10 workstation and depended on the RMS error criterion for convergence. It is clear that the final EOS data would not be able to go through the same processing and that faster inversion routines must be found to make this approach practicable for the EOS data information system. We therefore are also trying to reduce the number of parameters in the model to less than three.

5.1. Algorithm using Two Parameters (with Limits) CSAR Model

MISR does not measure in the principle plane, therefore: one may argue that a parameter which models forward or backward scattering (hot spot) (e.g. Θ_0 for the CSAR model) should not be used. Thus we modified the CSAR BRDF and set the term $F(g)$ in eq.(1) to unity.

This step improved the retrieval of the TOA albedo for bright and Lambertian surfaces which often showed erroneous hot-spots or specular peaks. In order to keep the parameters ϱ_0 and κ within their limits specified by CSAR, a variable transform from the original unbound variable ϱ_0 to the interval limited variable ϱ'_0 was used:

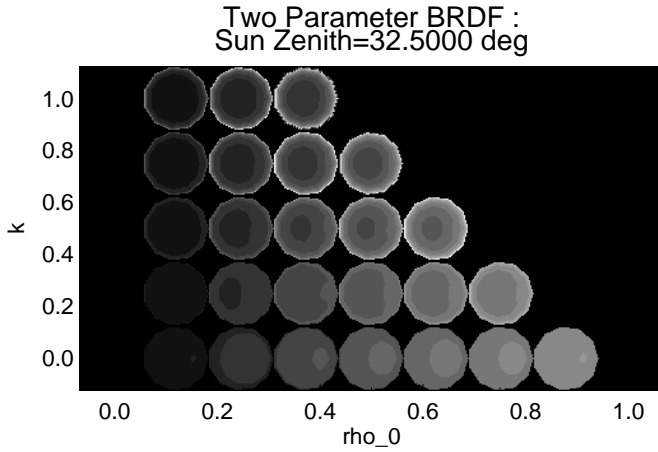


Figure 2: Polar representation of the two parameter BRDF for $\theta_s = 32.5^\circ$ and as a function of ϱ_0 and κ ($F(G) = 1$ and $\alpha < 1$).

$\varrho'_0 = \frac{1}{2} + \frac{\tan^{-1}(\varrho_0)}{\pi}$ and it's inverse: $\varrho_0 = \tan(\pi(\varrho'_0 - \frac{1}{2}))$. Similarly κ can be transformed to κ' . The BRDF used was given by:

$$BRF_{CSAR-mod}(\theta_i, \phi_i) = BRF_{CSAR}(\theta_i, \phi_i; \varrho'_0, \kappa', F(g) = 1). \quad (2)$$

The resulting standard deviations for various surface types are shown in Figure 3. The method works well for all cases and channels ($\sigma < 3.8\%$) For more typical MISR azimuthal angles between 30° and 60° the albedo errors are below 2% which is very good.

6. CONCLUSIONS

We find that for most cases our albedo error will be less than 1% in the visible and less than 1.5% in the NIR which is a significant advancement of the state-of-the-art for global change research goals. In contrast, if only nadir measurements are used the albedo error is about 5 % in the visible and 10 % in the NIR. More work is however needed to make this approach robustly work for all surfaces and atmospheric conditions.

7. ACKNOWLEDGMENTS

This work was supported by the Multi-angle Imaging Spectro Radiometer (MISR) project through a contract from NASA/JPL. We recognize the significant contributions by Dr. Carmen Tornow (DLR, Berlin), Dr. Veronique Carrère (JRC, Ispra) and Heather Stephens (LANL) and Kerstin Lippert (LANL and DLR, Berlin).

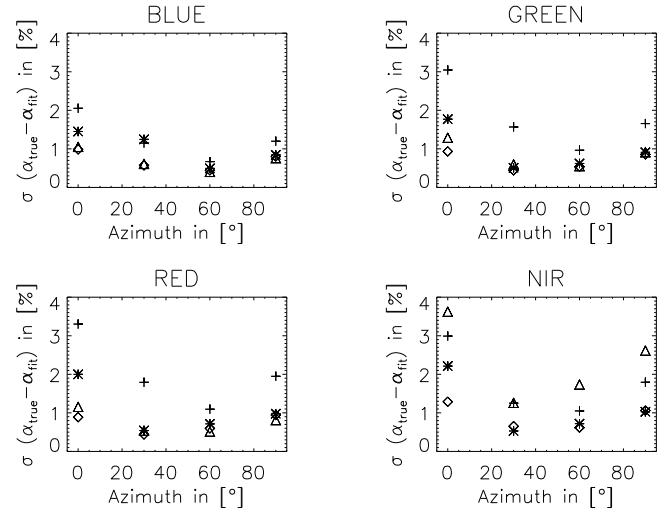


Figure 3: Standard deviation of the albedo error for a version of the parameter limited CSAR BRDF without the hot spot parameter Θ for various surface types (Symbols are described in section 5).

8. REFERENCES

- Abreu L.W., Chetwynd J.H., Anderson G.P. and Kimball L.M., 1995, MODTRAN 3 Scientific Report. Draft Preprint, Geophysics Laboratory, Air Force Command, US Air Force, Hanscom AFB, MA, USA.
- Diner D.J., Clothiaux E., Conel J.E., Davies R., Di Girolamo L., Muller J.-P., Varnai T. and Wenkert D., 1994, MISR Level 2 Algorithm Theoretical Product: TOA/Cloud Product, JPL Report D-11399, March 3.
- Kimes D.S. and Sellers P.J., 1985, Inferring hemispherical reflectance of the earth's surface for global energy budgets from remotely sensed nadir or directional radiance values, Remote Sens. Environ., 18, pp.205-223.
- Martonchik J.V., 1994, personal communication.
- Nicodemus F.E., Richmond J.C., Hsia J.J., Ginsberg I.W. and Limperis T., 1977, Geometrical Considerations and Nomenclature for Reflectance, Washington, D.C.: NBS Monograph 160, National Bureau of Standards, Dept. of Commerce, p.52.
- Rahman H., Verstraete M.M. and Pinty B., 1993, Coupled Surface-Atmosphere Reflectance (CSAR) Model (parts 1 and 2), JGR, 98:D11:20,779-20,789 and 98:D11:20,791-20,801.
- Vermote E., Tanré D., Deuzé J.L., Herman M. and Morcrette J.J., 1994, Second Simulation of the Satellite Signal in the Solar Spectrum, 6S User Guide, NASA-Goddard Space Flight Center, Greenbelt, USA, P 182.